Polynucleotide Functionalized Upconversion Nanoparticles for DNA Biosensoring

P. Alonso-Cristobal[a], *E. Lopez-Cabarcos*[a], *A. El-Sagheer*[b], *T. Brown*[b], *O. Muskens*[c], *J. Rubio-Retama*[a] *and A. G. Kanaras*[c]

[a] Department of Physical Chemistry II, Faculty of Pharmacy, Complutense University of Madrid, 28040 Madrid, Spain.

b

Department of Chemistry, University of Oxford

Chemistry Research Laboratory, Oxford, OX1 3TA United Kingdom

[c] Faculty of Physical Sciences and Engineering, University of Southampton, SO17 1BJ, United Kingdom.

KEYWORDS: Upconversion nanoparticles, graphene oxide, FRET, DNA Biosensor.

Correspondence to: bjrubio@ucm.es or a.kanaras@soton.ac.uk

Einem großen Freund und wunderbaren Mentor, gewidmet anlaesslich seines 65 Geburtstages. Schönen Geburtstag!

ABSTRACT:

In this work we prepared a DNA biosensor based on Fluorescence Resonance Energy Transfer (FRET) between upconversion nanoparticles (UCNPs), that act as donors, and

and graphene oxide (GO) that behaves as acceptor. The UCNPs were synthesized and functionalized with single strands of DNA (ssDNA). When UCNPs are in the proximity of the GO surface the interaction π-π stacking between the nucleobases of the DNA and the sp^2 carbons of the GO provokes the fluorescence quenching due to the overlapping between the fluorescence emission of the UCNPs and the absorption spectrum of GO. By contrast, in presence of the complementary and antiparallel DNA strands, the DNA strands anchored on the UCNPs self assemble with the complementary DNA chains rendering double DNA strands (dsDNA) that do not interact with the GO and thus the UCNPs recover their fluorescence. Our results demonstrate that this sensor can detect qualitatively and quantitatively the complementary DNA with a limit of detection in the range of femtomoles. Moreover, this sensor is sequence-specific and does not detect a random or non-complementary DNA sequence, whatever their concentration. The high sensitivity and the high specificity of this sensor will permit fast and reliable detection of bacterial, viral or human DNA and/or RNA.

INTRODUCTION

DNA is a biopolymer that can self assemble in a unique manner according to the Watson-Crick base pairing rules. This self-assembly between two complementary polymer chains, known as hybridization, is very specific and is based on the cooperative hydrogen bonds produced between the base pairs, rendering a double helix structure. This self-assembly capacity has been of great value in nanotechnology as a structural material in DNA origami,[1] polyhedral structures,[2] nanomechanical devices,[3] and as a template for the self-assembly of other materials such as gold nanoparticles.[4-6] This hybridization process has also been of great utility in biomedicine for applications in sensors.[7] The specificity of the self-assembly between complementary DNA strands can be used for the detection of certain sequences of interest related to viral[8] or bacterial[9] infections as well as in the detection of specific human DNA or mRNA sequences for the diagnosis of diseases[10] or mutations.[11]

Among others, biosensors based on quenching and turn on of fluorescence have shown significant advantages when were used as molecular beacons for amplified detection of metal ions and organic molecules.[12-14] These assays are designed with an Energy

Transfer (ET) pair in which the fluorescence of the donor is effectively quenched by the acceptor. The addition of complementary target DNA or RNA provokes a separation between the donor and the acceptor and therefore the fluorescence of the donor is turned-on proportionally to the concentration of the target. The sensing of DNA using these assays is often based on a self-complementary sequence within a hairpin loop that creates an intimate contact between the quencher and the fluorescent dye. Upon the addition of the complementary DNA, the hybridization provokes a separation of the fluorophore from the quencher and the fluorescence can be detected.[15-17] Other assays can detect the activity of DNAase enzymes which can selectively cleave a specific oligonucleotide sequence, thus separating the fluorophore from the quencher and restoring the fluorescence.[18] Although there are many strategies for the design of DNA based sensors, the detection sensitivity is determined by the fluorophores. The commonly used organic dyes suffer from photobleaching and inorganic quantum dots suffer from blinking effects. However, the main drawback is the excitation wavelength of these fluorophores, which is normally located in the UV-Vis region. Furthermore, the fluorescence background originating from biomolecules [19] and the inner filter effect provoked by the absorption of other species[20] limit the detection sensitivity. These drawbacks could be overcome using upconversion nanoparticles (UCNPs) as fluorescence donors.

The UCNPs are lanthanide doped inorganic materials in which the excitation wavelength is higher than the emission wavelength.[21,22] They have shown several advantages as fluorescence probes due to their high chemical and photochemical stability, low toxicity, large Stokes shifts, lack of photobleaching and absence of blinking.[23-27] However, the most important feature that makes the UCNPs an alternative to classical organic dyes is the excitation wavelength, which is located in the "Near-Infrared (NIR) region (typically 980 nm) which is the "optical transparency window" of biological tissues.[28] This excitation wavelength does not provoke any autofluorescence of the biomolecules and also produces lower light scattering compared with UV-Vis radiation.[29] For these reasons, the signal to noise ratio can be greatly enhanced by using these UCNPs as biological labels.[30] It is important to note that the upconversion fluorescence is produced by the inner 4f-4f orbital electronic transitions that are shielded by the outer complete 5s and 5p orbitals, and the quenching of this fluorescence is only possible on the surface of the particles.[31] For this reason, the

upconversion fluorescence would require nanoparticles in which the surface-related effects are dominant. However, an effective quencher for upconversion fluorescence is difficult to find.[32] Among others[33,34], water soluble graphene oxide has been used as an ultra-highly efficient quencher for UCNPs when the nanoparticles are in intimate contact with the GO surface.[35] For this to happen, it would be necessary to functionalize the UCNPs with molecules capable of interacting attractively with the GO surface. It has been demonstrated that ssDNA biopolymers have a strong affinity for the surface of GO due to strongly attractive π-π interactions between the nitrogenous nucleobases and the highly unsaturated structure of graphene oxide.[36] In contrast, dsDNA has all the base pairs hybridized and therefore they do not interact with the graphene oxide surface. On this basis, it should be possible to design a fluorescence sensor for DNA using UCNPs and GO as a FRET pair. Such upconversion fluorescence probes would be functionalized with ssDNA and should be highly monodisperse and small enough to permit FRET with graphene oxide. In the presence of the complementary DNA strand (cDNA) the hybridization process would lead to dsDNA and the upconversion fluorescence would be detectable.

In this work we prepared a fluorescence DNA sensor platform using the FRET pair formed by Upconversion Nanoparticles (UCNPs) as fluorophores and Graphene Oxide (GO) as quencher. We used erbium and ytterbium doped β-$NaYF_4$ nanoparticles as the fluorescent donor because it is one of the most efficient upconverting nanomaterials.[37] The ratio between the ssDNA functionalized UCNPs and GO was optimized for obtaining the maximum sensitivity and the biosensor was evaluated using the cDNA sequence at different concentrations. In addition, the hybridization conditions for the self-assembly of the DNA sequences were studied as a function of temperature and a strong relationship was found between these conditions and the sensitivity of the sensor. The experimental results demonstrate that this sensor permits the detection of cDNA with a great sensitivity and specificity with a fast and reproducible methodology. This platform could be used with biological DNA or RNA target sequences related to a specific diseases or mutations.

EXPERIMENTAL SECTION

Materials. Erbium(III) chloride hexahydrate (99.9%), Ytterbium(III) chloride hexahydrate (99.9%), Yttrium(III) chloride hexahydrate (99.99%), 1-Octadecene (80%),

Oleic acid (90%), Sodium hydroxide (98%), Ammonium fluoride (98%), Methanol (99.9%), *n*-Hexane (95%), *N*,*N*-Dimethylformamide anhydrous (DMF) (99.8%), Tetraethyl orthosilicate (TEOS) (99.999%), Polyoxyethylene (5) nonylphenylether, branched (IGEPAL CO-520), Ammonium hydroxide solution (30%), (3-Aminopropyl)triethoxysilane (APTES) (99%), Succinic anhydride (99%), Phosphate buffered saline tablets, *N*-(3-Dimethylaminopropyl)-*N*´-ethylcarbodiimide hydrochloride (EDC) (99%) and *N*-Hydroxysulfosuccinimide sodium salt (Sulfo-NHS) (98%) were purchased from Sigma-Aldrich (St. Louis, USA) and used as received. Nano Graphene oxide (powder) was purchased from Graphene Supermarket Inc (New York, USA). The phosphate buffered saline (PBS) solutions were prepared dissolving the tablet following the manufacturer's specifications.

The DNA sequences were obtained from ATDBio (School of Chemistry, University of Southampton, UK). The ssDNA sequence that was covalently linked to the surface of the nanoparticles (named from now on as probe ssDNA sequence) was 5´-aminohexyl-TTTTTTTTTTTTTTTTTTTT-3´. The target sequence (named from now on as complementary ssDNA sequence) was 5´-AAAAAAAAAAAAAAA-AAAAAAAAAAAAAAA-3´. The random sequence (named from now on as non-complementary ssDNA sequence) was 5´-CTAGATCCGTGTCCTCGT-3´. All the DNA oligomers were purified by reversed phase HPLC and the concentration was calculated with UV-Vis spectroscopy.

Synthesis of monodisperse $NaYF_4$:Yb,Er nanoparticles. The synthesis was performed by following a previously reported procedure[38,39] with slight modifications: 236.62 mg of Yttrium(III) chloride hexahydrate (0.78 mmol), 77.5 mg of Ytterbium(III) chloride hexahydrate (0.20 mmol) and 7.63 mg of Erbium(III) chloride hexahydrate (0.02 mmol) were dissolved in a three-necked round bottom flask with 6 mL of oleic acid (19 mmol) and 15 mL of 1-octadecene (46.9 mmol) and heated at 160 ºC for 1 hour and 30 minutes under nitrogen atmosphere. After this time, a solution containing 100 mg of sodium hydroxide (2.5 mmol) and 148.16 mg of ammonium fluoride (4 mmol) dissolved in 10 mL of methanol was added dropwise under vigorous stirring. This mixture was slowly heated to 100 ºC for two hours under nitrogen atmosphere and then 30 more minutes under vacuum. Next, the flask containing the mixture was set up with a thermometer, a reflux condenser and nitrogen atmosphere, and placed in a heating mantle. The temperature was raised to 300 ºC and left to react for 1 hour and 30

minutes. Subsequently, the mixture was left to cool down to room temperature and the $NaYF_4$:Yb,Er nanoparticles were collected by centrifugation (8500 rpm, 10 minutes) with a mixture of hexane, ethanol and water (2:1:1 in volume). The pellet was redispersed with 5 mL of ethanol and centrifuged in a mixture of ethanol and water (1:1 v/v). This process was repeated three times. Finally, the purified $NaYF_4$:Yb,Er nanoparticles were redispersed and stored in hexane.

Synthesis of $NaYF_4$:Yb,Er@SiO_2 nanoparticles. The silica coating of the synthesized UCNPs was performed by the base catalyzed polymerization of TEOS in a reverse microemulsion.[40,41] Briefly, 240 mg of IGEPAL CO-520 and 5 mL of a hexane solution with the UCNPs (2 mg/mL) were mixed with an ultrasound bath. Then, 40 µL of ammonium hydroxide solution (30%) were added and gently mixed. The solution turned totally transparent, which indicated the formation of the microemulsion. The reaction started when 30 µL of TEOS were added under stirring, and it was left to react overnight at room temperature. The reaction finished when the microemulsion was destabilized with 5 mL of methanol. The core@shell $NaYF_4$:Yb,Er@SiO_2 nanoparticles (UCNPs@SiO_2) were purified by centrifugation (8500 rpm, 10 min) with ethanol three times.

Surface modification of the $NaYF_4$:Yb,Er@SiO_2 nanoparticles. The carboxylic acid functionalized $NaYF_4$:Yb,Er@SiO_2 nanoparticles (UCNPs@SiO_2-COOH) were prepared by sequential functionalization steps[43]: First, the surface was functionalized with amino groups by the addition of 150 µL of APTES to the synthesized UCNPs@SiO_2 dissolved in 5 mL of ethanol. This mixture was stirred at room temperature overnight. The UCNPs@SiO_2-NH_2 nanoparticles were centrifuged and dispersed in 5 mL of anhydrous DMF three times. Then, 150 mg of succinic anhydride (1.49 mmol) were dissolved in 3 mL of anhydrous DMF and added dropwise to the anhydrous DMF solution containing the UCNPs@SiO_2-NH_2 and stirred at room temperature overnight. The ring opening reaction led to the carboxylic acid functionalized upconversion@silica nanoparticles, which were collected by centrifugation. The DMF solvent traces were removed after several centrifugation steps with ethanol. Finally, the UCNPs@SiO_2-COOH nanoparticles were dispersed in water.

Attachment of the probe ssDNA sequence to the $NaYF_4$:Yb,Er@SiO_2 nanoparticles. The DNA was covalently attached to the surface of the nanoparticles by

the carbodiimide coupling reaction. This reaction produced a covalent bond between the carboxylic acid group on the surface of the UCNPs@SiO_2 nanoparticles and the amino group in the 5´ end of the probe ssDNA sequence. The EDC coupling reaction was performed as follows: The UCNPs@SiO_2-COOH nanoparticles were dispersed in borate buffered solution (0.001 M) at a concentration of 1.82 mg/mL. 200 µL of this solution (0.364 mg of nanoparticles) were added to an eppendorf tube prior to the addition of 20 µL of an EDC solution in borate buffer (0.3 M) and 40 µL of a Sulfo-NHS solution in borate buffer (0.3 M). The mixture was shaken for 5 minutes and then 30 µL of the aqueous solution of probe ssDNA (220.65 µM) were added. The reaction was stirred overnight and the probe ssDNA functionalized nanoparticles (UCNPs@SiO_2-ssDNA) were purified by centrifugation (16.400 rpm, 20 minutes) twice. The purified UCNPs@SiO_2-ssDNA nanoparticles were collected with phosphate buffered saline (PBS) solution (0.01 M pH 7.4) and stored at -20 ºC.

Characterization methods. TEM specimens of the nanoparticles were prepared by placing a drop of a diluted solution on a TEM copper grid coated with a Formvar film and left to dry in air. The size and morphology of the samples were observed with a JEM-1010 electron microscope working at 80 kV equipped with a digital camera GATAN megaview II (JEOL, Japan). The nanoparticle size distribution was analyzed with ImageJ (National Institutes of Health, USA) and Soft Imaging Viewer (Olympus, Japan) software, considering over 300 nanoparticles for the statistical analysis. The upconversion fluorescence measurements were performed in a manually aligned setup with a continuous wave 980 nm 500 mW diode laser (Armlaser, USA) as excitation source and a SpectraSuite Spectrometer (OceanOptics, USA) as detector. The detector was placed at an angle of 90º to the excitation beam, and the emitted fluorescence was collected via fiber optic cable and measured with the software provided by SpectraSuite (OceanOptics, USA). A cuvette with the corresponding solvent was measured under illumination with the 980 nm laser beam and set as the blank for each measurement. All measurements were performed with 2.000 msec of integration time and 100 scans to average. All fluorescence experiments were repeated at least three times with independent measurements and the fitted data presented in this manuscript shows the statistically significant mean value ± error. The represented data (graphs) represent one individual measurement for an easier visualization. The Z-potential measurements were performed using a Zetasizer Nano ZS instrument (Malvern Instruments, UK) and the

accumulation time was determined automatically for each sample. The acquired data was processed using the software provided by Malvern (Zetasizer software v7.03).

RESULTS AND DISCUSSION

Synthesis and surface functionalization of Upconversion Nanoparticles. The synthesis of $NaYF_4$:Yb,Er nanoparticles produced highly monodisperse spherical UCNPs with a mean diameter of 29.1 ± 2.2 nm as measured by TEM micrographs (Figure 1A). These nanoparticles could be easily dispersed in organic solvents such as hexane due to the presence of oleic acid as capping and stabilizing agent. The UCNPs were subsequently coated with a silica shell by a reverse microemulsion method. With this procedure it was possible to obtain monodisperse spherical core@shell $NaYF_4$:Yb,Er@SiO_2 nanoparticles in which each upconversion nanoparticle was covered with silica and no large aggregates with multiple-core were found. The overall mean diameter of the UCNPs@SiO_2 nanoparticles was 47.34 ± 3.8 nm with a silica shell thickness of approximately 11 nm as analyzed with TEM micrographs (Figure 1B). The UCNPs@SiO_2 nanoparticles could be dispersed in polar solvents such as ethanol or water. The obtained nanoparticles showed the characteristic upconversion fluorescence spectrum for Ytterbium and Erbium doped $NaYF_4$ nanoparticles when excited with a CW 980 nm 500 mW laser diode (Figure 1C). The upconversion fluorescence with these Erbium doped nanoparticles showed the emissions at 534 and 549 nm (green emission corresponding to the transition $^4S_{3/2} \rightarrow {}^4I_{15/2}$) and at 654 nm (red emission corresponding to the transition $^4F_{9/2} \rightarrow {}^4I_{15/2}$).[42] The nanoparticles dispersed in water formed a transparent solution in which the upconversion fluorescence could be observed by the naked eye when the sample was excited with the 980 nm laser (Figure 1D).

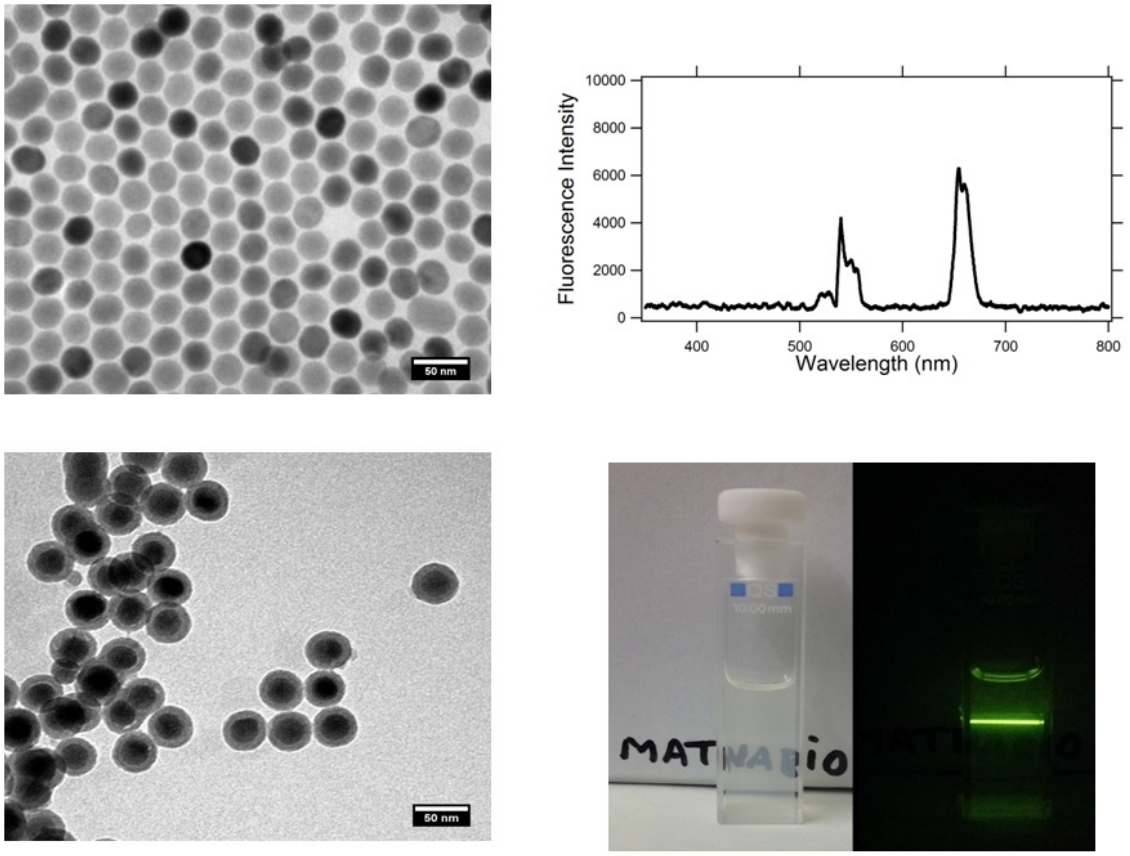

Figure 1. A) TEM micrograph of monodisperse $NaYF_4$:Yb,Er nanoparticles. B) TEM micrograph of monodisperse and individually coated $NaYF_4$:Yb,Er@SiO_2 nanoparticles. Scale bars are 50 nm. C) Fluorescence spectrum of a diluted solution in ethanol of the silanized upconversion nanoparticles when excited with a cw 980 nm laser. D) Pictures taken of the diluted solution of silanized upconversion nanoparticles in ethanol without laser excitation (left) and the same solution under the excitation of a cw 980 nm laser (right). The room light was turned off to take this picture.

The surface of the $NaYF_4$:Yb,Er@SiO_2 nanoparticles was then modified in several steps prior to the covalent attachment of the ssDNA sequence (Scheme 1).

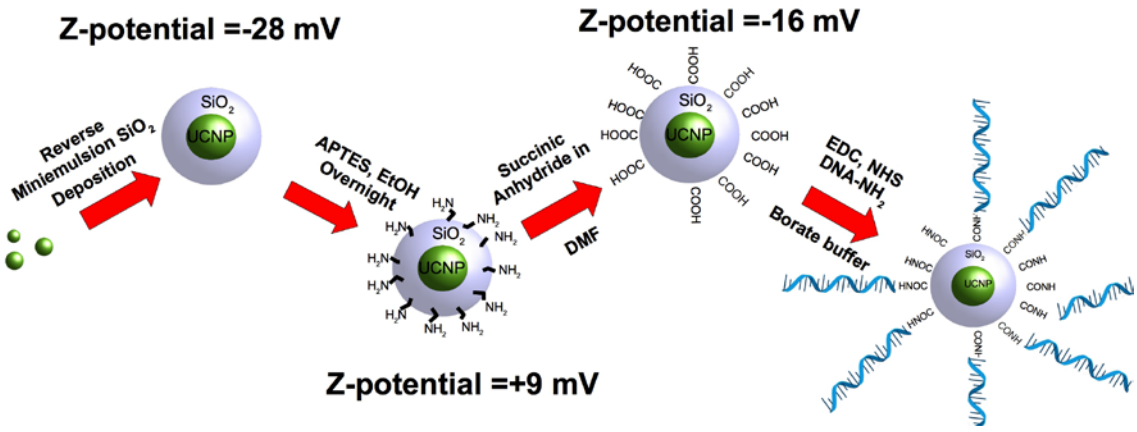

Scheme 1. Synthetic pathway for the functionalization of UCNPs@SiO_2 nanoparticles. The first step resulted in silanization of the upconversion nanoparticles. Then, the surface was positively charged with amino groups with APTES. These amino groups acted as nucleophiles for the reaction with succinic anhydride, which led to carboxylic acid functionalized UCNPs@SiO_2 nanoparticles. The final step consisted in the EDC coupling reaction between the amino-modified probe ssDNA sequence and the obtained carboxylic acid in the surface of the nanoparticles.

The first functionalization step consisted in the addition of an excess of (3-aminopropyl)triethoxysilane (APTES) to the nanoparticles in ethanol. The Z-potential of the UCNPs@SiO_2 nanoparticles turned from -28.3 ± 3.55 mV to +8.74 ± 3.99 mV which was indicative of the presence of NH_2 groups on the surface of the nanoparticles (named UCNPs@SiO_2-NH_2). The variation of the Z-potential was concomitant with a reduction of the aqueous stability of these nanoparticles. This step provided amino groups, which could act as nucleophilic centers for the reaction with succinic anhydride in DMF. This ring opening reaction created a covalent amide bond and a terminal carboxylic acid group in the surface of the nanoparticles. After this reaction, the Z-potential changed from +8.74 ± 3.99 mV to -16.4 ± 3.99 mV indicating the presence of carboxylate groups. The resulting UCNPs@SiO_2-COOH nanoparticles were highly stable in aqueous solution. Figure 2 shows the Z-potential of the UCNPs@SiO_2, UCNPs@SiO_2-NH_2 and UCNPs@SiO_2-COOH nanoparticles respectively.

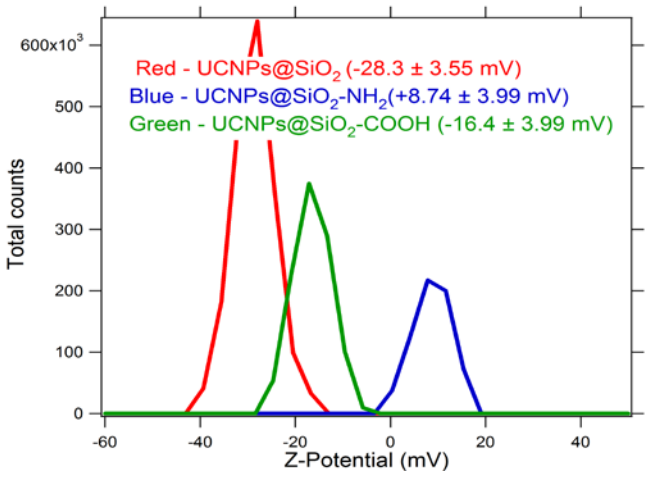

Figure 2. Z-potential measurements of the surface-functionalized upconversion nanoparticles: UCNPs@SiO_2 nanoparticles (red curve); UCNPs@SiO_2-NH_2 nanoparticles (blue curve); and UCNPs@SiO_2-COOH nanoparticles (green curve).

The presence of COOH groups on the surface of the UCNPs@SiO_2-COOH nanoparticle opens the possibility to covalently attach ssDNA by means of the EDC coupling reaction. With the appropriate buffered solution, and the co-activator Sulfo-NHS and EDC as catalysts, the 5´-amino modified ssDNA was attached, rendering the UCNPs@SiO_2-ssDNA nanoparticles. The probe ssDNA was used in excess in the synthesis so that the maximum quantity was attached. However, it was not possible to measure the total amount of ssDNA per nanoparticle. A control synthesis was performed with a similar sequence that contained a fluorescent dye (Cy3) at the 3´ end. The fluorescence of the Cy3 was observed after the purification steps, which indicated that the coupling was successful (Figure S1 in the Supporting Information).

Optimization and evaluation of the ssDNA sensor based on UCNPs and Graphene Oxide. The FRET pair between UCNPs@SiO_2-ssDNA and Graphene Oxide (GO) was studied for the optimization of the sensor. First, the concentration UCNPs@SiO_2-ssDNA nanoparticles was set as 0.4 mg/mL in 2 mL, and different concentrations of GO (ranging from 0 to 1 mg/mL) were prepared and incubated at 40 ºC for one hour. After this time, the samples were left to cool down to room temperature prior to the fluorescence measurements, figure 3 depicts the fluorescence intensity of the UCNPs@SiO_2-ssDNA as a function of the GO concentration.

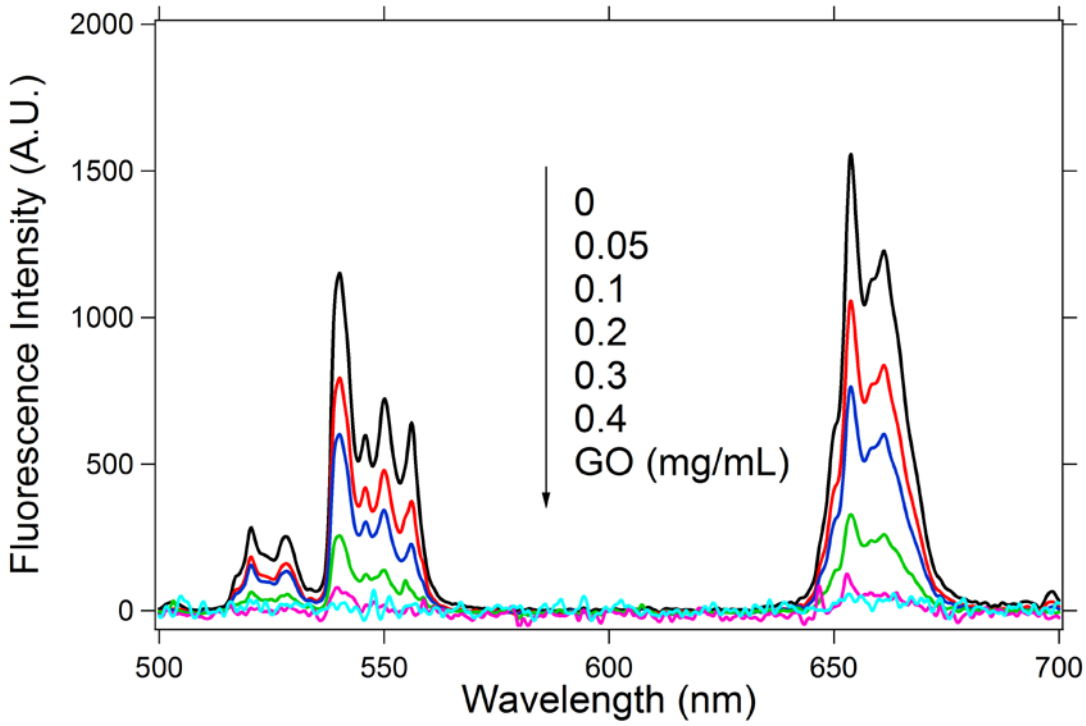

Figure 3. Upconversion fluorescence spectra of the UCNPs@SiO_2-ssDNA nanoparticles (0.4 mg/mL) in the presence of different concentrations of graphene oxide (exc. 980 nm).

Figure 3 depicts the reduction of fluorescence intensity of UCNPs@SiO_2-ssDNA (0.4 mg/mL) when the concentration of graphene oxide increased. The analysis of the fluorescence quenching of UCNPs@SiO_2-ssDNA at 549 nm and 654 nm as a function of the GO concentration is shown in figure 4.

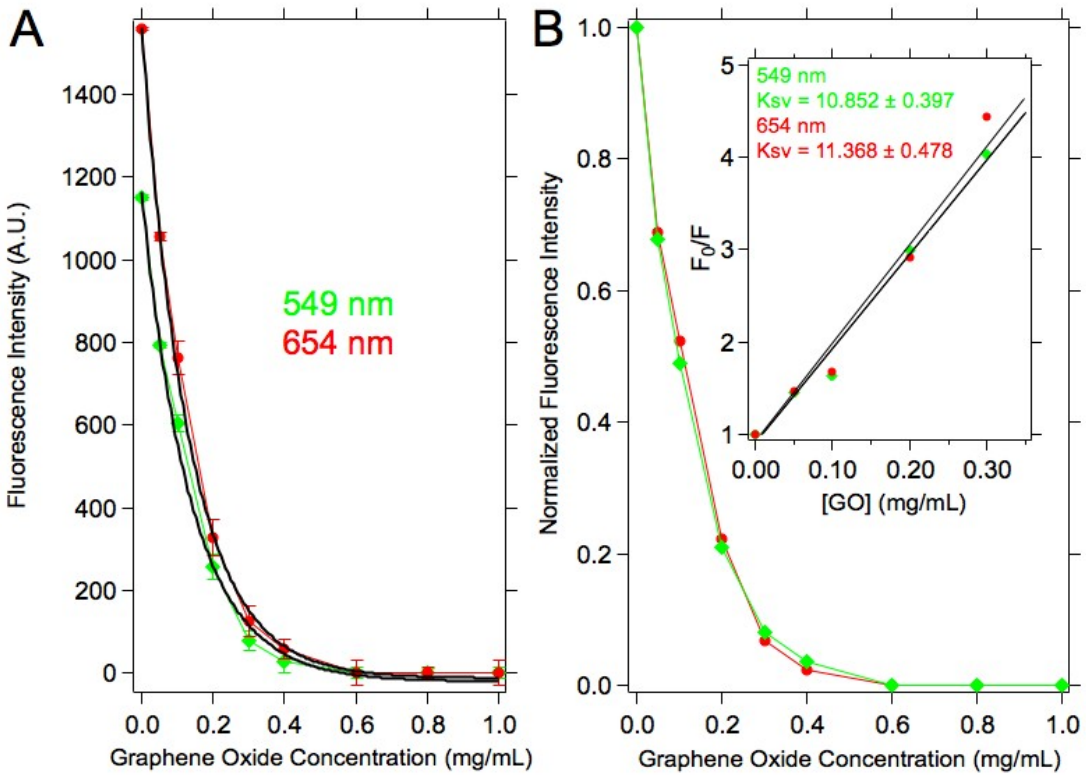

Figure 4. Representation of A) the maximum fluorescence intensity and B) normalized fluorescence intensity of the UCNPs (0.4 mg/mL) measured at 549 and 654 nm as a function of the GO concentration. The inset in figure 4B) represents the Stern−Volmer plot for the fluorescence quenching with GO of the emission bands located at 549 nm (green line) and 654 nm (red line) respectively.

Figure 4A shows that the fluorescence intensity was almost quenched when the concentration of GO was around 0.3 mg/mL. From this point, a further addition of GO provoked a very small increase in quenching. This behavior was equal for both Erbium emission wavelengths located at 549 and 654 nm respectively, as is shown in figure 4B. These results permitted us to establish 0.3 mg/mL of GO as the optimum concentration for quenching the fluorescence emission of 0.4 mg/ml of the UCNPs@SiO_2-ssDNA since it was the minimum concentration of quencher that provoked the maximum fluorescence decrease. A quantitative measure of the fluorescence quenching is given by the Stern−Volmer constant K_{SV}, defined by:

$$F_0/F=1+K_{sv}\cdot[GO]$$

where F_0 and F are the intensities of fluorescence in the absence and in the presence of the quencher, respectively, and [*GO*] is the concentration of quencher.

For the UCNPs@SiO_2-ssDNA quenched by GO the obtained K_{sv} was around 11 for both wavelengths, indicating that the quenching mechanism was due to FRET between the UCNPs and the GO, and not by a simple absorption process in which the GO would absorb the photons emitted by the UCNPs. If this was the case, the fluorescence quenching of the photons at 549 nm would have been higher than that of the photons at 654 nm, due to the absorption spectrum of GO (Figure S2 in the Supporting Information).

With the aim to assess the importance of the interaction between the ss-DNA and GO on the fluorescence quenching of the UCNPs@SiO_2-ssDNA, the fluorescence of UCNPs@SiO_2 with and without ssDNA at a concentration of 0.4 mg/mL was studied in the presence of 0.3 mg/ml of GO (see figure 5).

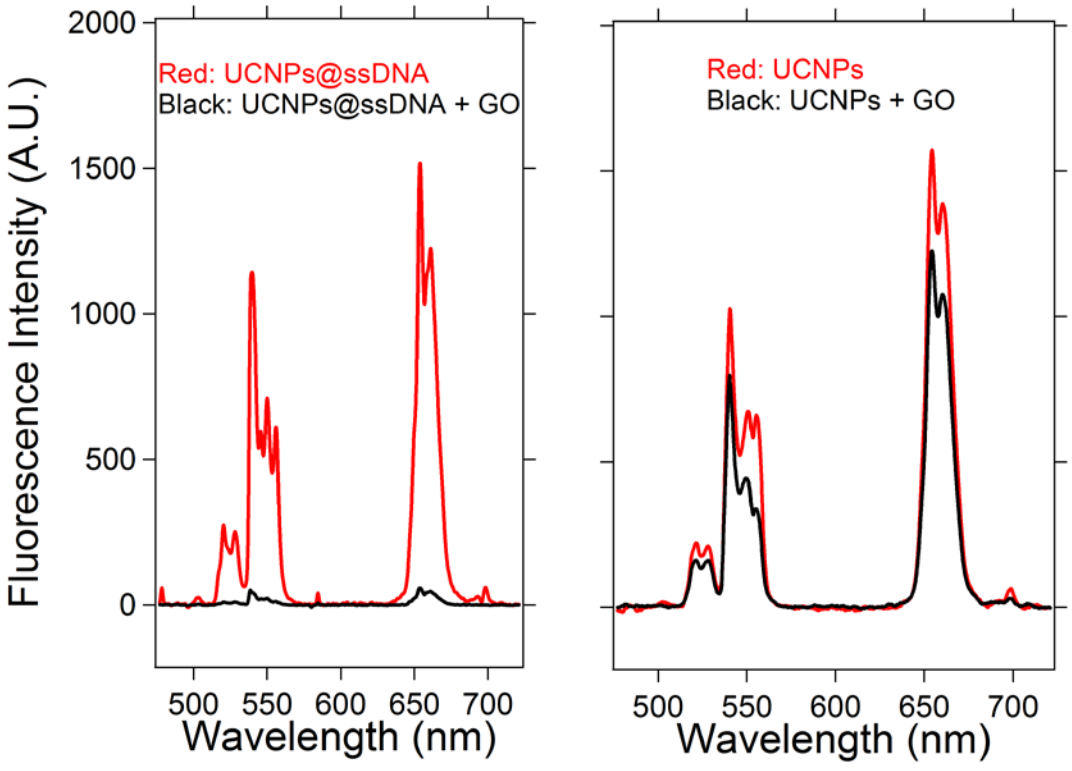

Figure 5. Left: Fluorescence intensity of 0.4 mg/mL of UCNPs@SiO_2-ssDNA nanoparticles in the presence (black curve) and in the absence (red curve) of 0.3 mg/mL of GO. Right: Fluorescence intensity of 0.4 mg/mL of UCNPs@SiO_2 nanoparticles in the presence (black

curve) and in the absence (red curve) of 0.3 mg/mL of GO. Both samples were incubated for 1 hour at 40 ºC.

The control experiments demonstrated that 0.3 mg/mL of GO was able to quench the 97% of the fluorescence emission of the UCNPs@SiO_2-ssDNA. By contrast, under the same experimental conditions, the fluorescence quenching observed on UCNPs@SiO_2 nanoparticles without DNA was around 16%. These results demonstrated that the FRET based fluorescence quenching was specific for UCNPs@SiO_2-ssDNA nanoparticles and was due to the attractive π-π interactions between the ssDNA and the GO surface.

A means to disrupt the attractive π-π interactions between the ssDNA and the GO surface could be hybridization of the ssDNA strand with its complementary ssDNA sequence, which could be the target molecule. That would induce a conformational change of the DNA strands that would prevent the adsorption of the UCNPs@SiO_2-ssDNA nanoparticles on the GO surface. As result the UCNPs@SiO_2-ssDNA nanoparticles would recover their fluorescence. In order to prove this, 0.4 mg/mL of UCNPs@SiO_2-ssDNA nanoparticles were incubated in PBS with different concentrations of the complementary ssDNA (from 0.1 nM to 400 nM) for 2 minutes at 90 ºC and then slowly cooled down to 40 ºC. After this time, a solution of GO in PBS was added and the final concentration was 0.3 mg/mL. The mixture was incubated for 1 hour at 40 ºC and then cooled down to room temperature prior to performing the fluorescence measurements. Figure 6 represents the fluorescence intensity of UCNPs@SiO_2-ssDNA nanoparticles in the presence of GO and different concentrations of the complementary ssDNA.

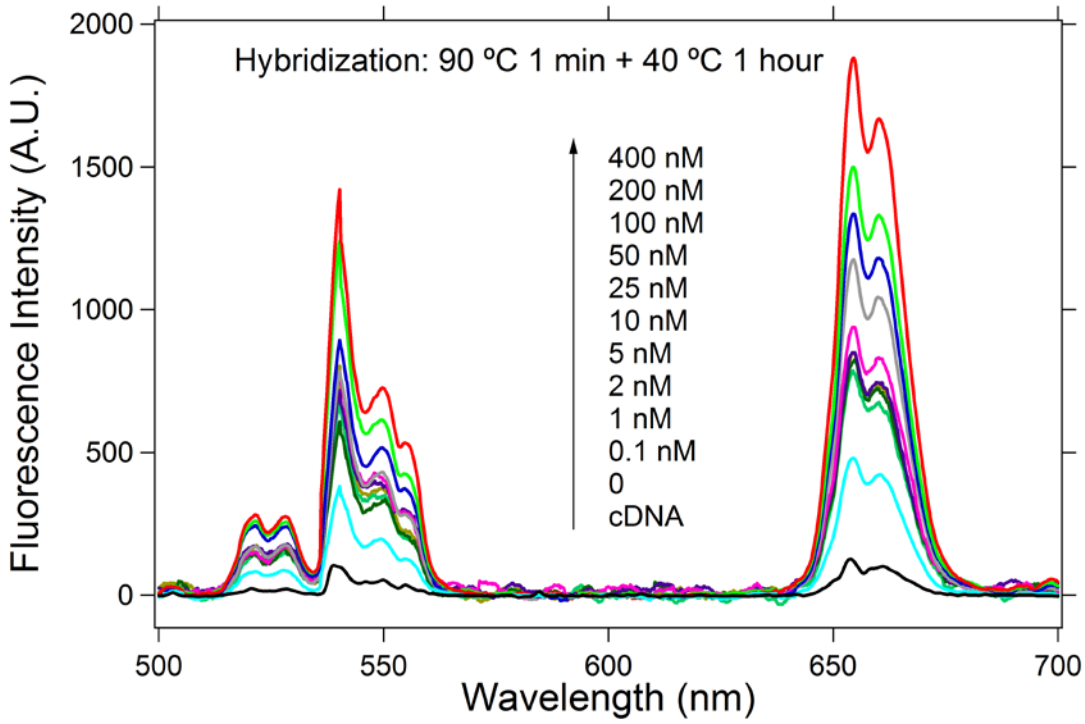

Figure 6. Representation of the fluorescence spectra of the UCNPs@SiO_2-ssDNA nanoparticles (0.4 mg/mL) in the presence of different concentrations of complementary ssDNA and 0.3 mg/mL of GO (red curves) The black curve is the fluorescence spectrum without the addition of complementary ssDNA. (exc 980 nm)

Figure 6 shows the fluorescence intensity recovery of the UCNPs@SiO2-ssDNA nanoparticles in the presence of GO after adding increasing concentrations of the complementary ssDNA. The analysis of the maximum intensity as a function of the concentration of the complementary ssDNA is represented in figure 7.

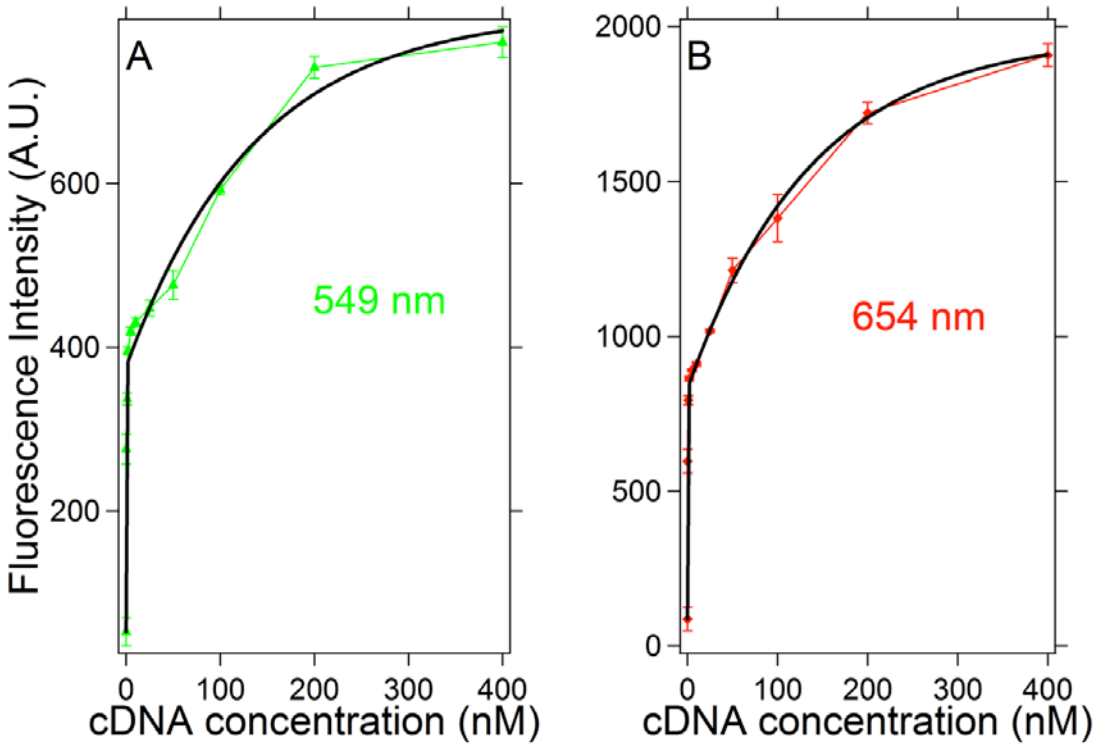

Figure 7. Representation of the maximum fluorescence intensity bands measured at 549 nm (left) and 654 nm (right) of the UCNPs@SiO_2-ssDNA nanoparticles as a function of the complementary ssDNA concentration.

Figure 7 shows two trends in the fluorescence recovery upon the addition of the complementary ssDNA strands. Thus, at low concentrations of complementary ssDNA (below 2 nM) the intensity recovery increases abruptly. This increment could be due to the contribution of those UCNPs@SiO2-ssDNA nanoparticles functionalized with the fewest number of ssDNA strands, which can be hybridized completely, even at low concentrations of DNA. As result, these particles do not interact with the surface of GO and recover their fluorescence intensity. By contrast, for those particles functionalized with larger numbers of ssDNA strands it is necessary to add higher concentrations of complementary ssDNA. Under this scenario, the ssDNA strands anchored on the surface of the nanoparticles can be completely hybridized and the fluorescence intensity totally recovered

The fluorescence intensity measured with the highest concentration of complementary ssDNA (400 nM) was almost equal to that of the solution of UCNPs@SiO_2-ssDNA (0.4 mg/mL) without GO and no further increments were observed after increasing even

more the concentration of the complementary ssDNA. This result would indicate that under this condition, the UCNPs@SiO_2-ssDNA would be totally hybridized.

The detection limit of this DNA biosensor was experimentally demonstrated to be at a concentration of 100 pM. However, the theoretical detection limit inferred from the double exponential fitting function was 5 pM. Taking into account that the total volume of the sample solutions was 2 mL, the amount of complementary DNA detected in our experiments was 100 fmoles.

The specificity of the sensor was evaluated with a control experiment, in which the UCNPs@SiO_2-ssDNA nanoparticles (0.4 mg/mL) were incubated in PBS in the presence of non-complementary DNA sequences at concentrations from 100 nM to 1μM. The incubation was performed at 90 ºC for 2 minutes and then a PBS solution of GO was added, obtaining a final concentration of 0.3 mg/mL, and left for 1 hour at 40 ºC. After cooling down to room temperature, the upconversion fluorescence was measured, see Figure 8.

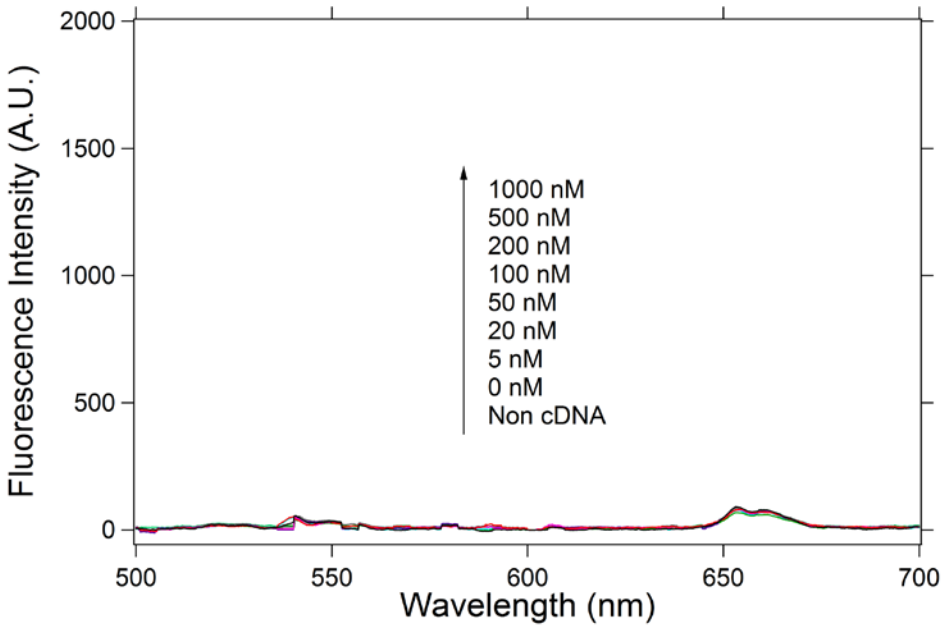

Figure 8. Representation of the upconversion fluorescence spectra of the UCNPs@SiO_2-ssDNA nanoparticles (0.4 mg/mL), hybridized at 90 ºC for 2 minutes and at 40 ºC for 1 hour, with different concentrations of a random sequence of ssDNA (non complementary ssDNA) and 0.3 mg/mL of GO (red curves).

Figure 8 shows that independently of the concentration of non-complementary DNA strands, the UCNPs@SiO_2-ssDNA did not recover their fluorescence emission, which

remained constant in the same range of values as the intensity obtained for UCNPs@SiO_2-ssDNA (0.4 mg/mL) totally quenched with GO (0.3 mg/mL). These results demonstrate that this DNA biosensor platform is selective for its complementary DNA strand.

CONCLUSIONS

In this work a DNA biosensor platform was prepared by exploiting the FRET pair formed between upconversion nanoparticles and graphene oxide. The UCNPs were synthesized and functionalized with ssDNA on the surface. The quenching of the upconversion fluorescence was demonstrated to be specific for the ssDNA functionalized nanoparticles. The influence of the ratio between the concentration of the UCNPs@SiO_2-ssDNA nanoparticles and the concentration of GO was studied and optimized. When the nanoparticles were incubated with fully complementary DNA, the fluorescence was not quenched by the GO. The fluorescence intensity depended on the cDNA concentration. This should permit the use of this biosensor platform in both qualitative and quantitative assays. The detection limit was experimentally and theoretically calculated to be in the pM range, which corresponded in our experimental conditions to femtomoles of cDNA. In addition, it was demonstrated that the sensor was sequence-specific. To the best of our knowledge, this is the first FRET pair that reports such a high sensitivity and specificity for DNA sensing.

ACKNOWLEDGEMENTS

Authors acknowledge the Spanish Ministry of Science for the project MAT2010-15349 and the Juan Palomo Foundation (YMGYMC-01-2014) for the financial support. Paulino Alonso-Cristobal acknowledges the Spanish Ministry of Education for the FPU grant AP2010-1163. Patrick Vilela acknowledges (whatever).

REFERENCES

(1) Rothemund, P. W. K. Folding DNA to create nanoscale shapes and patterns. *Nature* **2006**, 440, 297-302.

(2) He, Y.; Ye, T.; Su, M.; Zhang, C.; Ribbe, A. E.; Jiang, W.; Mao, C. Hierarchical self-assembly of DNA into symmetric supramolecular polyhedral. *Nature* **2008**, 452, 198-201.

(3) Yan, H.; Zhang, X.; Shen, Z.; Seeman, N. C. A robust DNA mechanical device controlled by hybridization topology. *Nature* **2002**, 415, 62-65.

(4) Le, J. D.; Pinto, Y.; Seeman, N. C.; Musier-Forsyth, K.; Taton, A. T.; Kiehl, R. A. DNA-templated self-assembly of metallic nanocomponent arrays on a surface. *Nano Letters* **2004**, 4 (12), 2343-2347.

(5) Zhang, J.; Liu, Y.; Ke, Y.; Yan, H. Periodic square-like gold nanoparticle arrays templated by self-assembled 2D DNA nanogrids on a surface. *Nano Letters* **2006**, 6 (2), 248-251.

(6) Ding, B.; Deng, Z.; Yan, H.; Cabrini, S.; Zuckermann, R. N.; Bokor, J. Gold nanoparticle self-similar chain structure organized by DNA origami. *J. Am. Chem. Soc.* **2010**, 132, 3248-3249.

(7) Niemeyer, C. M.; Adler, M. Nanomechanical devices based on DNA. *Angew. Chem. Int. Ed.* **2002**, 41 (20), 3779-3783.

(8) Wang, J.; Cai, X.; Rivas, G.; Shiraishi, H.; Farias, P. A. M.; Dontha, N. DNA electrochemical biosensor for the detection of short DNA sequences related to the human immunodeficiency virus. *Anal. Chem.* **1996**, 68, 2629-2634.

(9) Mao, X.; Yang, L.; Su, X. L.; Li, Y. A nanoparticle amplification based quartz crystal microbalance DNA sensor for detection of Escherichia coli O157:H7. *Biosensors and Bioelectronics* **2006**, 21, 1178-1185.

(10) Liu, G.; Wan, Y.; Gau, V.; Zhang, J.; Wang, L.; Song, S.; Fan, C. An enzyme-based E-DNA sensor for sequence-specific detection of femtomolar DNA targets. *J. Am. Chem. Soc.* **2008**, 130, 6820-6825.

(11) Marrazza, G.; Chiti, G.; Mascini, M.; Anichini, M. Detection of human Apolipoprotein E genotypes by DNA electrochemical biosensor coupled with PCR. *Clinical Chemistry* **2000**, 46 (1), 31-37.

(12) Zhang, X. B.; Wang, Z.; Xing, H.; Xiang, Y.; Lu, Y. Catalytic and molecular beacons for amplified detection of metal ions and organic molecules with high sensitivity. *Anal. Chem.* **2010**, 82, 5005-5011.

(13) Liu, X.; Tan, W. A fiber-optic evanescent wave DNA biosensor based on novel molecular beacons. *Anal. Chem.* **1999**, 71, 5054-5059.

(14) Nutiu, R.; Li, Y. Structure-switching signaling aptamers. *J. Am. Chem. Soc.* **2003**, 125, 4771-4778.

(15) Du, H.; Disney, M. D.; Miller, B. L.; Krauss, T. D. Hybridization-based unquenching of DNA hairpins on Au surfaces: Prototypical "molecular-beacon" biosensors. *J. Am. Chem. Soc.* **2003**, 125, 4012-4013.

(16) Bonnet, G.; Krichevsky, O.; Libchaber, A. Kinetics of conformational fluctuations in DNA hairpin-loops. *Proc. Natl. Acad. Sci.* **1998**, 95, 8602-8606.

(17) Zhang, J.; Qi, H.; Li, Y.; Yang, J.; Gao, Q.; Zhang, C. Electrogenerated chemiluminescence DNA biosensor based on hairpin DNA probe labeled with ruthenium complex. *Anal. Chem.* **2008**, 80, 2888-2894.

(18) Suzuki, M.; Husimi, Y.; Komatsu, H.; Suzuki, K.; Douglas, K. T. Quantum dot FRET biosensors that respond to pH, to proteolytic or nucleolytic cleavage, to DNA synthesis, or to a multiplexing combination. *J. Am. Chem. Soc.* **2008**, 130, 5720-5725.

(19) Chen, Z.; Chen, H.; Hu, H.; Yu, M.; Li, F.; Zhang, Q.; Zhou, Z.; Yi, T.; Huang, C. Versatile synthesis strategy for carboxylic acid-functionalized upconverting nanophosphors as biological labels. *J. Am. Chem. Soc.* **2008**, 130, 3023-3029.

(20) Frangioni, J. V. In vivo near-infrared fluorescence imaging. *Current Opinion in Chemical Biology* **2003**, 7, 626-634.

(21) Mai, H. X.; Zhang, Y. W.; Sun, L. D.; Yan, C. H. Highly efficient multicolor up-conversion emissions and their mechanisms of monodisperse $NaYF_4$:Yb,Er core and core/shell structured nanocrystals. *J. Phys. Chem. C* **2007**, 111, 13721-13729.

(22) Binnemans, K. Lanthanide-based luminescent hybrid materials. *Chem. Rev.* **2009**, 109, 4283-4374.

(23) Niagara, M. I.; Muthu, K. G.; Zhang, J.; Ho, P. C.; Mahendran, R.; Zhang, Y. In vivo photodynamic therapy using upconversion nanoparticles as remote-controlled nanotransducers. *Nature Medicine* **2012**, 18 (10), 1580-1585.

(24) Xu, C. T.; Svenmarker, P.; Liu, H.; Wu, X.; Messing, M. E.; Wallenberg, L. R.; Andersson-Engels, S. High-resolution fluorescence diffuse optical tomography developed with nonlinear upconverting nanoparticles. *ACS Nano* **2012**, 6 (6), 4788-4795.

(25) Wang, Y. F.; Liu, G. Y.; Sun, L. D.; Xiao, J. W.; Zhou, J. C.; Yan, C. H. Nd^{3+}-sensitized upconversion nanophosphors: Efficient in vivo bioimaging probes with minimized heating effect. *ACS Nano* **2013**, 7 (8), 7200-7206.

(26) Yan, B.; Boyer, J. C.; Habault, D.; Branda, N. R.; Zhao, Y. Near infrared light triggered release of biomacromolecules from hydrogels loaded with upconversion nanoparticles. *J. Am. Chem. Soc.* **2012**, 134, 16558-16561.

(27) Chen, G.; Qiu, H.; Prasad, P. N.; Chen, X. Upconversion nanoparticles: Design, nanochemistry, and applications in theranostics. *Chem. Rev.* **2014**, 114, 5161-5214.

(28) Chatterjee, D. K.; Rufaihah, A. J.; Zhang, Y. Upconversion fluorescence imaging of cells and small animals using lanthanide doped nanocrystals. *Biomaterials* **2008**, 29, 937-943.

(29) Huang, X.; El-Sayed, I. H.; Qian, W.; El-Sayed, M. A. Cancer cell imaging and photothermal therapy in the near-infrared region by using gold nanorods. *J. Am.Chem. Soc.* **2006**, 128, 2115-2120.

(30) Li, Z.; Zhang, Y.; Jiang, S. Multicolor core/shell-structured upconversion fluorescent nanoparticles. *Adv. Mater.* **2008**, 20, 4765-4769.

(31) Zhang, H.; Li, Y.; Ivanov, I. A.; Qu, Y.; Huang, Y.; Duan, X. Plasmonic modulation of the upconversion fluorescence in $NaYF_4$:Yb/Tm hexaplate nanocrystals using gold nanoparticles or nanoshells. *Angew. Chem.* **2010**, 122, 2927-2930.

(32) Rantanen, T.; Järvenpää, M. L.; Vuojola, J.; Kuningas, K.; Soukka, T. Fluorescence-quenching-based enzyme-activity assay by using photon upconversion. *Angew. Chem. Int. Ed.* **2008**, 47, 3811-3813.

(33) Li, Z.; Wang, L.; Wang, Z.; Liu, X.; Xiong, Y. Modification of $NaYF_4$:Yb,Er@SiO_2 nanoparticles with gold nanocrystals for tunable green-to-red upconversion emissions. *J. Phys. Chem. C* **2011**, 115, 3291-3296.

(34) Wu, T.; Wilson, D.; Branda, N. R. Fluorescent quenching of lanthanide-doped upconverting nanoparticles by photoresponsive polymer shells. *Chem. Mater.* **2014**, 26, 4313-4320.

(35) Liu, C.; Wang, Z.; Jia, H.; Li, Z. Efficient fluorescence resonance energy transfer between upconversion nanophosphors and graphene oxide: a highly sensitive biosensing platform. *Chem. Commun.* **2011**, 47, 4661-4663.

(36) Wang, Y.; Li, Z.; Hu, D.; Lin, C. T.; Li, J.; Li, Y. Aptamer/graphene oxide nanocomplex for in situ molecular probing in living cells. *J. Am. Chem. Soc.* **2010**, 132, 9274-9276.

(37) Liu, C.; Wang, H.; Li, X.; Chen, D. Monodisperse, size tunable and highly efficient β-$NaYF_4$:Yb,Er(Tm) up-conversion luminescent nanospheres: controllable synthesis and their surface modifications. *J. Mater. Chem.* **2009**, 19, 3546-3553.

(38) Li, Z.; Zhang, Y. An efficient and user-friendly method for the synthesis of hexagonal-phase $NaYF_4$:Yb,Er/Tm nanocrystals with controllable shape and upconversion fluorescence. *Nanotechnology* **2008**, 19, 345606-345611.

(39) Qian, H. S.; Guo, H. C.; Ho, P. C. L.; Mahendran, R.; Zhang, Y. Mesoporous-silica-coated up-conversion fluorescent nanoparticles for photodynamic therapy. *Small* **2009**, 20 (5), 2285-2290.

(40) Han, Y.; Jiang, J.; Lee, S. S.; Ying, J. Y. Reverse microemulsion-mediated synthesis of silica-coated gold and silver nanoparticles. *Langmuir* **2008**, 24, 5842-5848.

(41) Serrano-Ruiz, D.; Alonso-Cristobal, P.; Mendez-Gonzalez, D.; Laurenti, M.; Olivero-David, R.; López-Cabarcos, E.; Rubio-Retama, J.; Nanosegregated Polymeric Domains on the Surface of Fe_3O_4@SiO_2 Particles, . *J. Polymer Sci. Part A,* **2014**, 52, 2966–2975.

(42) Yi, G.; Sun, B.; yang, F.; Chen, D.; Zhou, Y.; Cheng, J. Synthesis and characterization of high-efficiency nanocrystal up-conversion phosphors: Ytterbium and Erbium codoped Lanthanum Molybdate. *Chem. Mater.* **2002**, 14, 2910-2914.

(43) Vaz, A. M.; Serrano-Ruiz, D.; Laurenti, M, Alonso-Cristobal, P.; Lopez-Cabarcos, E.; Rubio-Retama, J.; Synthesis and characterization of biocatalytic gamma-Fe_2O_3@SiO_2 particles as recoverable bioreactors, *Colloids and Surface B-BIOINTERFACES*, **2014**, 114, 11-19

TOC